

Paramagnetic Resonance Absorption in Two Sulfates of Copper*

ROBERT D. ARNOLD AND ARTHUR F. KIP

Research Laboratory of Electronics, Massachusetts Institute of Technology, Cambridge, Massachusetts

(Received December 13, 1948)

Resonance absorption measurements in $\text{CuSO}_4 \cdot 5\text{H}_2\text{O}$ and $\text{CuK}_2(\text{SO}_4)_2 \cdot 6\text{H}_2\text{O}$ exhibit dissimilarities caused by different degrees of exchange coupling between paramagnetic ions. In the single salt, in which the ions are more closely spaced, exchange coupling causes the absorption lines to be much narrower than would be predicted on the basis of ordinary magnetic dipolar broadening, and causes the appearance of a single line in cases where two lines should otherwise be found. Neither of these effects is observed in the double salt.

I. INTRODUCTION

RESONANCE absorption of radiation by paramagnetic ions in a static magnetic field has been investigated at this laboratory in two salts of copper. This type of experiment was first reported by Zavoisky¹ and later by Cummerow, Halliday, Moore and Wheatley²⁻⁴ and Weiss, Whitmer, Torrey, and Hsiang.^{5,6}

In the present experiments the widths and positions of absorption lines in single crystals of $\text{CuSO}_4 \cdot 5\text{H}_2\text{O}$ and $\text{CuK}_2(\text{SO}_4)_2 \cdot 6\text{H}_2\text{O}$ were determined for various orientations of the crystal in the static magnetic field. Measurements were also made on powders of the two salts. All of these measurements were at room temperature and at a wave-length of about 3.25 cm.

The magnetic characteristics of an ion in a solid, influenced by the electric field due to the surrounding atoms, can be quite different from the properties of the same ion in the free state.⁷ If a Cu^{++} ion is situated in an electric field of sufficient strength and of sufficiently low symmetry, the lowest energy level has only a twofold spin degeneracy and is separated from the next higher level by an interval large compared to KT at room temperature.⁸ This results in an effective partial quenching of the orbital contribution to the magnetic moment. Also, the magnitude of the splitting in an external magnetostatic field of the degeneracy in the lowest level is determined by the spin quantum number, S , rather than the total angular momentum quantum

number, J . The splitting factor, g , is given by

$$g = p/[S(S+1)]^{\frac{1}{2}}, \quad (1)$$

where p is the effective magnetic moment of the ion in units of the Bohr magneton. This factor multiplied by the Bohr magneton, β , and the external magnetic field, H , gives the magnetic splitting

$$h\nu = g\beta H. \quad (2)$$

In cases where the symmetry of the electric field is less than cubic, the value of p is a function of the orientation of the electric field with respect to the magnetic field. The value of g can also be affected by exchange coupling between magnetic ions (see §III D).

It has been shown experimentally¹⁻⁶ and theoretically⁹ by others that if the ions are subjected to an alternating magnetic field at right angles to H there will be observable resonance absorption at the frequency ν in Eq. (2), provided relaxation conditions are favorable.

II. EXPERIMENTAL METHOD

A. Microwave Equipment

The paramagnetic crystal is placed at the center of a rectangular microwave resonant cavity which is driven in the TE_{102} mode. This central position is the point of maximum r-f magnetic field and minimum r-f electric field and is therefore the position affording maximum sensitivity in magnetic absorption measurements. The cavity is placed between the pole faces of an electromagnet in such a way that the oscillating magnetic field is orthogonal to the magnetostatic field H .

An iris of adjustable aperture couples the cavity to one side arm of a wave-guide magic T whose other side arm is terminated in a matched load. (The load is matched to about 1.01 $VSWR$ at each operating frequency by means of a calibrated tuning screw.) The other two magic T arms are connected through matched attenuators, respectively, to a reflex klystron and to a crystal detector. The de-

* This work has been supported in part by the Signal Corps, the Air Materiel Command, and the Office of Naval Research.

¹ E. Zavoisky, *J. Phys. U.S.S.R.* **10**, 197 (1946).

² R. L. Cummerow and D. Halliday, *Phys. Rev.* **70**, 433 (1946).

³ R. L. Cummerow, D. Halliday, and G. E. Moore, *Phys. Rev.* **72**, 1233 (1947).

⁴ J. Wheatley, D. Halliday, and J. H. Van Vleck, *Phys. Rev.* **74**, 1211 (1948).

⁵ P. R. Weiss, C. A. Whitmer, H. C. Torrey, and J. S. Hsiang, *Phys. Rev.* **72**, 975 (1947).

⁶ P. R. Weiss, *Phys. Rev.* **73**, 470 (1948).

⁷ J. H. Van Vleck, *The Theory of Electric and Magnetic Susceptibilities* (Oxford University Press, London, 1932), p. 282.

⁸ D. Polder, *Physica* **9**, 709 (1942).

⁹ J. Frenkel, *J. Phys. U.S.S.R.* **9**, 299 (1945).

tected signal is then proportional to the power reflected from the cavity which is, to a good approximation, related to the cavity Q by

$$P_r = \left\{ \frac{Q_e/Q_0 - 1}{Q_e/Q_0 + 1} \right\}^2 P_i, \quad (3)$$

where P_i is the power incident on the cavity, P_r is the reflected power, Q_e is the external Q , and Q_0 is the unloaded Q of the cavity. The external Q will be unaffected by the magnetostatic field, while the reciprocal unloaded Q will be proportional to the sum of the electrical and magnetic losses in the cavity. By observing P_r as a function of the magnitude of H and by using Eq. (3), one can obtain the relative magnetic absorption as a function of H . To check the constancy of P_i , readings of P_r for zero-applied magnetic field are taken before and after each run.

The experimental procedure follows. The iris is adjusted, with the sample crystal in place in the cavity and no static magnetic field applied, so that P_r/P_i is roughly 0.1 at resonance. The klystron

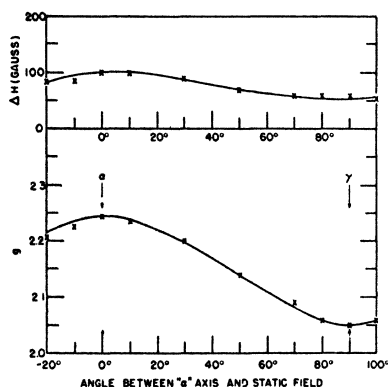


FIG. 1. Line width (ΔH) and splitting factor (g) in $\text{CuSO}_4 \cdot 5\text{H}_2\text{O}$ single crystal, static field perpendicular to β -axis, $\lambda = 3.244$ cm.

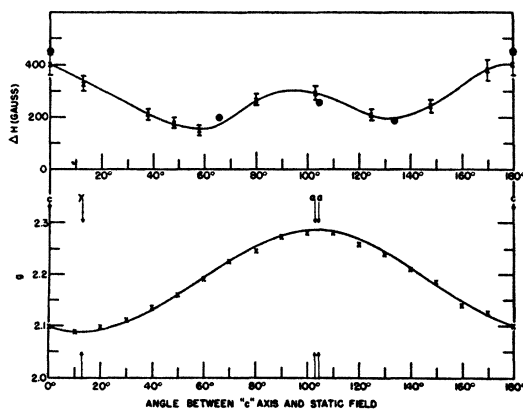


FIG. 2. Line width (ΔH) and splitting factor (g) in $\text{CuK}_2(\text{SO}_4)_2 \cdot 6\text{H}_2\text{O}$ single crystal, static field perpendicular to b -axis, $\lambda = 3.259$ cm. The points indicated by \bullet are calculated from Van Vleck's theory of dipolar broadening (see §IV C).

TABLE I. Calculated g values.

	$\text{CuSO}_4 \cdot 5\text{H}_2\text{O}$	$\text{CuK}_2(\text{SO}_4)_2 \cdot 6\text{H}_2\text{O}$
g_{11}	$2.38 \pm .02$	$2.42 \pm .02$
g_{\perp}	$2.05 \pm .01$	$2.09 \pm .01$
φ	41° ^a	$40.5^\circ \pm 1^\circ$
g_α	2.245	2.285
g_β	2.20	2.24
g_γ	2.05	2.09
g_{11} (susc.)	2.47 ^b	2.42 ^c
g_{\perp} (susc.)	2.07 ^b	2.05 ^c
$F_5 - F_3$	$34,000 \pm 5500 \text{ cm}^{-1}$	$19,000 \pm 3000 \text{ cm}^{-1}$
$F_4 - F_3$	$18,000 \pm 1000 \text{ cm}^{-1}$	$16,000 \pm 900 \text{ cm}^{-1}$

^a See reference 10.

^b See reference 11.

^c See reference 8.

is square-wave modulated with the carrier frequency at the cavity resonant frequency. The detector signal is applied to an amplifier tuned to the fundamental of the square-wave modulation and the amplifier output is read on a meter. For each setting of the static magnetic field the oscillator frequency is adjusted for minimum reflection from the cavity. This is important because the magnetic resonance not only affects the Q of the cavity but slightly changes the cavity resonant frequency. This frequency shift is negligible compared to the width of the magnetic absorption, but is sometimes appreciable compared to the width of the cavity resonance. Frequency is measured by means of a resonant cavity wavemeter. Meter reading (relative reflected power) as a function of the magnitude of H is then recorded.

In the case of the two salts reported here, the meter reading for very high magnetic field was the same as for zero field, indicating the absence of zero-field magnetic absorption.

B. Measurement of Magnetic Field

A rotating coil, driven by a synchronous motor, is placed in the magnetic field. The generated 30-c.p.s. voltage is connected in series with a 3000-c.p.s. voltage, controlled by a calibrated potentiometer, and the resultant signal is applied to an oscilloscope with a 60-c.p.s. sweep. The oscilloscope pattern serves as an accurate null indicator and the magnetic field strength is proportional to the potentiometer reading at null setting.

The device is calibrated by comparison with a TS 15A/AP fluxmeter. Calibration is checked by measuring the field of a permanent magnet before and after each run. The TS 15A/AP was found by comparison with a proton resonance measurement (in Professor F. Bitter's laboratory at M.I.T.) to read 2.0 percent high. This correction in the field value has not been made in Figs. 3 and 4, but it has been included in the calculation of the g values. Error in measurement of the magnetic field is estimated to be ± 0.5 percent.

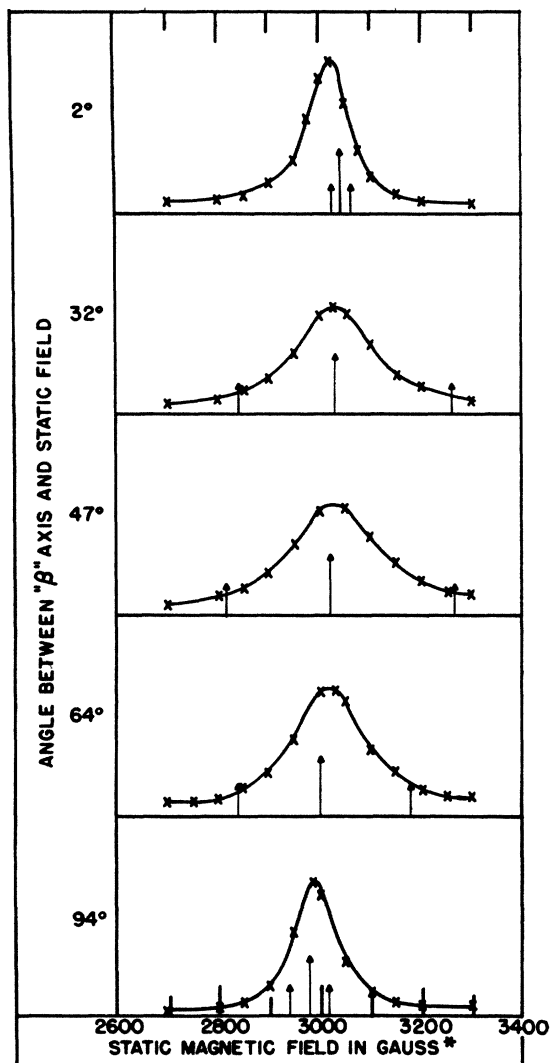


FIG. 3. Resonance absorption lines in $\text{CuSO}_4 \cdot 5\text{H}_2\text{O}$ single crystal, static field perpendicular to γ -axis, $\lambda = 3.260$ cm. Short arrows indicate line positions expected in the absence of exchange interaction; long arrows indicate positions expected with strong interaction. (*Actual magnetic field values are 2.0 percent less than indicated here. See §II B.)

C. Crystal Orientation

The sample crystal is oriented on an optical goniometer and then transferred to the cavity in such a way that its orientation with respect to the cavity is known. The crystal is fastened with polystyrene cement to a rotatable polystyrene shaft which is perpendicular to H . A pointer and dial indicate the shaft position. After a series of runs on a given crystal, the crystal and its holder can be transferred from the cavity back to the goniometer and the orientation rechecked. Over-all error in orientation is about $\pm 2^\circ$.

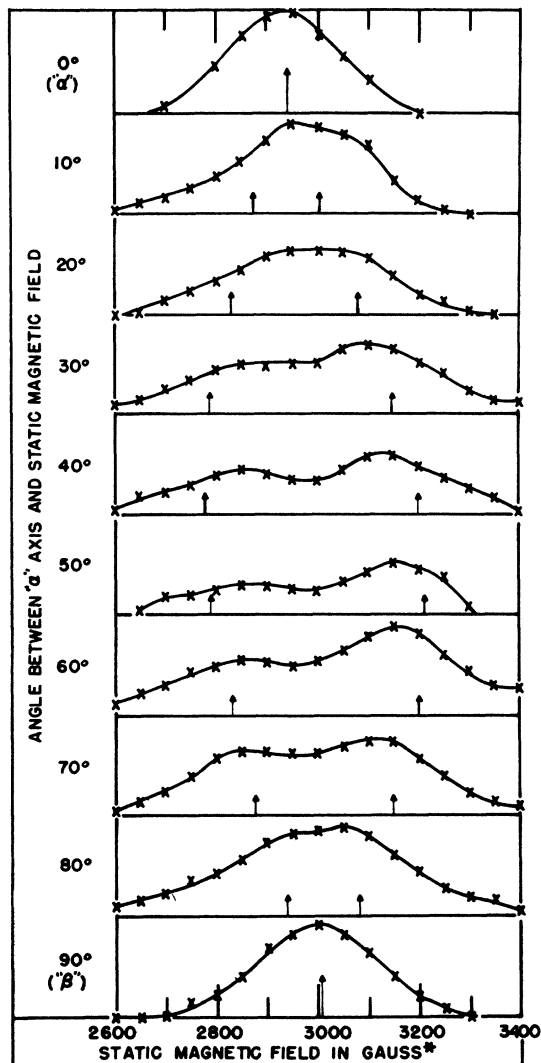


FIG. 4. Resonance absorption lines in $\text{CuK}_2(\text{SO}_4)_2 \cdot 6\text{H}_2\text{O}$ single crystal, static field perpendicular to γ -axis, $\lambda = 3.254$ cm. Arrows indicate line positions expected in the absence of exchange interaction. (*Actual magnetic field values are 2.0 percent less than indicated here. See §II B.)

III. COPPER SULFATE

A. Crystal Form

From x-ray measurements, Beevers and Lipson¹⁰ find that each of the two Cu^{++} ions in the unit cell of $\text{CuSO}_4 \cdot 5\text{H}_2\text{O}$ is located at the center of an octahedron formed by four water molecules at the corners of a square and two oxygen ions along a line perpendicular to the square and passing through its center. The oxygen ions are slightly more distant from the Cu^{++} than are the water molecules. Small deviations from regularity of the octahedron are neglected here. As a result of this configuration,

¹⁰ C. A. Beevers and H. Lipson, Proc. Roy. Soc. London A146, 570 (1934).

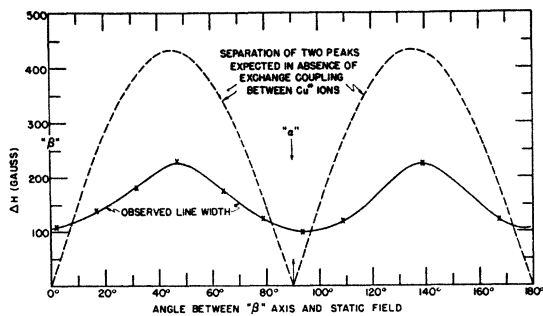


FIG. 5. Line widths in $\text{CuSO}_4 \cdot 5\text{H}_2\text{O}$ single crystal, static field perpendicular to γ -axis, $\lambda = 3.260$ cm.

each Cu^{++} ion is at the center of an electric field of tetragonal symmetry, the tetragonal axis passing through the two oxygens. Susceptibility measurements by Krishnan and Mookherji¹¹ verify the angular relationships between the tetragonal axes and the crystallographic axes derived from the x-ray data. (We define the magnetic axes as in Eq. (5a) which makes our α, β, γ correspond to γ, β, α of Krishnan and Mookherji.) Orientations of crystallographic axes with respect to crystal faces are taken from Dana.¹²

Polder⁸ has calculated the splitting of the Cu^{++} ground state (2D) in a tetragonal electric field and the effect of the splitting on the magnetic moment of the ion. He finds that

$$\begin{aligned} g_{\parallel} &= 2[1 - (4\lambda/(F_4 - F_3))], \\ g_{\perp} &= 2[1 - (\lambda/(F_5 - F_3))], \end{aligned} \quad (4)$$

where “ \parallel ” and “ \perp ” refer to the orientation of the tetragonal axis with respect to the external magnetic field H ; λ is $\lambda(L \cdot S)$, the spin-orbit coupling energy in the ion, F_3 the energy of the lowest level of the 2D state split by a tetragonal field, and F_4 and F_5 are two higher levels.

The tetragonal axes associated with the two Cu^{++} ions are oriented 82° apart. Calling these axes Z_I and Z_{II} , the axes of principal susceptibility are $\alpha =$ bisector of the acute angle between Z_I and Z_{II} , $\beta =$ bisector of the obtuse angle between Z_I and Z_{II} , $\gamma =$ normal to plane of Z_I and Z_{II} ,

$$(5a)$$

and the g values in these three directions are

$$\begin{aligned} g_{\alpha}^2 &= g_{\parallel}^2 \cos^2 \varphi + g_{\perp}^2 \sin^2 \varphi, \\ g_{\beta}^2 &= g_{\parallel}^2 \sin^2 \varphi + g_{\perp}^2 \cos^2 \varphi, \\ g_{\gamma} &= g_{\perp}, \end{aligned} \quad (5b)$$

where φ is one-half of the acute angle between Z_I and Z_{II} . In general, the g value of the ion associated with Z_i is

$$g_i^2 = g_{\parallel}^2 \cos^2 \theta_i + g_{\perp}^2 \sin^2 \theta_i, \quad (6)$$

where θ_i is the angle between Z_i and H .

¹¹ K. S. Krishnan and A. Mookherji, *Phys. Rev.* **54**, 533, 841 (1938).

¹² J. D. Dana, *Systems of Mineralogy* (John Wiley and Sons, Inc., New York, 1900), p. 944.

B. Measured g Values

A crystal of $\text{CuSO}_4 \cdot 5\text{H}_2\text{O}$ was mounted in the microwave cavity with its β -axis ($66^\circ, 85^\circ, 42^\circ$ from a, b, c) along the rotatable polystyrene rod, which is perpendicular to the magnetostatic field H . Using Eq. (2), g values were calculated from the magnetic resonances observed at different crystal rotation positions (Fig. 1). Values of g_{α} and g_{γ} were thus obtained and, since φ is known, g_{\parallel}, g_{\perp} , and g_{β} can be calculated from Eq. (5b). These values are listed in Table I. Listed for comparison are the g values obtained from susceptibility measurements.¹¹ If the susceptibility obeys the Curie law, the Curie constant, C , and g are related by

$$g[S(S+1)]^{\frac{1}{2}} = (3kC/N\beta^2)^{\frac{1}{2}} = 2.83(C)^{\frac{1}{2}}, \quad (7)$$

where $N =$ Avogadro's number, $\beta =$ the Bohr magneton, and $k =$ Boltzmann's constant. Included in the table are values of $F_5 - F_3$ and $F_4 - F_3$ from Eq. (4), letting $\lambda(L \cdot S)$ take on its free-ion value of -852 cm^{-1} .

C. Line Widths

From purely geometrical considerations, neglecting exchange interaction, there should be, in general, two resonance absorption peaks for a given orientation, since the axes Z_I and Z_{II} make different angles with H (see Eq. 6). However, for all positions of rotation of the crystal mounted with β normal to H , these two angles are equal and the absorption lines corresponding to the two Cu^{++} ions in the unit cell are, therefore, exactly superimposed. Under these conditions the line width at half-maximum absorption was found to vary from 55 gauss with the magnetostatic field parallel to the γ -axis to 100 gauss with the field parallel to the α -axis. This variation is shown in Fig. 1.

Van Vleck¹³ has calculated the line width to be expected from magnetic dipolar interaction alone and has shown that the addition of exchange interaction between the magnetic ions will have the effect of narrowing the line. In $\text{CuSO}_4 \cdot 5\text{H}_2\text{O}$ the “dipolar” line width would be approximately 475 gauss. The large discrepancy between this and the observed line widths is evidence that there is strong exchange interaction between the Cu^{++} ions in this salt.

D. Effect of Exchange Interaction on Line Position

If the sample crystal is mounted in the microwave cavity so that its γ -axis ($155^\circ, 68^\circ, 50^\circ$ from a, b, c) is along the rotatable shaft, there will be positions of rotation at which the axes Z_I and Z_{II} make different angles with H . Even so, only one absorption peak is observed. In Fig. 3 the observed

¹³ J. H. Van Vleck, *Phys. Rev.* **74**, 1168 (1948).

lines are shown for various angles of orientation. The small arrows indicate positions of the two peaks expected in the absence of exchange interaction, calculated from Eq. (6).

Theoretical considerations, according to Van Vleck,¹⁴ indicate that if there is sufficient exchange coupling between the two types of Cu^{++} ions (differently oriented electric fields) they will act as a single resonator with a g value which is the arithmetic mean of the values expected in the absence of exchange coupling. The long arrows in Fig. 3 are at positions corresponding to these mean values of g . It is possible that resolution of two peaks is prevented by the width of the individual lines, but the width of the combined line is small enough (230 gauss) so that the separation of the individual lines must be less than 25 percent of the separation expected in the absence of exchange coupling.¹⁵

In Fig. 5 the widths of the observed single lines are plotted as a function of crystal orientation. For comparison, there is also shown the separation of the two individual peaks expected in the absence of exchange coupling (short arrows in Fig. 3). Note that the minimum line widths occur where this separation is zero, and the maximum width at maximum separation.

E. Absorption in Powder

The absorption line in the powdered salt is an intergration over all directions of the line for a single crystal. In the absence of exchange coupling, the unit of integration would be the individual Cu^{++} ion and the powder absorption line would extend from $H(g_{11})$ to $H(g_{\perp})$. It would be peaked near $H(g_{\perp})$ because of the greater geometrical probability of the perpendicular orientation. If there is strong exchange coupling, however, the unit of intergration must be the complete unit cell having no g value higher than g_{α} . In this case the line should extend from $H(g_{\alpha})$ to $H(g_{\gamma})$ and should be peaked near $H(g_{\alpha})$, since the near equality of g_{α} , g_{β} , and all g values in the plane of α , β causes a high geometrical probability of this value of g . The observed powder absorption (Fig. 6) corresponds again to the strong coupling model.

IV. COPPER POTASSIUM SULFATE

A. Crystal Form

There is no x-ray information on the $\text{CuK}_2(\text{SO}_4)_2 \cdot 6\text{H}_2\text{O}$ salt, but in an x-ray investigation by Hof-

mann¹⁶ of similar salts, $\text{XY}_2(\text{SO}_4)_2 \cdot 6\text{H}_2\text{O}$, the ion corresponding to Cu^{++} was found to be located at the center of a water-oxygen octahedral complex which is analogous to that found in $\text{CuSO}_4 \cdot 5\text{H}_2\text{O}$. There are again two Cu^{++} ions in the unit cell and the axes Z_I and Z_{II} are differently oriented. (The postassium ion is diamagnetic.) Susceptibility measurements by Miss Hupse¹⁷ reveal that one of the magnetic axes in $\text{CuK}_2(\text{SO}_4)_2 \cdot 6\text{H}_2\text{O}$ is along the b - (ortho) axis and the other two lie in the plane of the a - and c -axes. The susceptibility experiment leaves an ambiguity as to which magnetic axis is the one normal to the plane of Z_I and Z_{II} ,⁸ but the resonance absorption experiment resolves the ambiguity (see §IV D). Orientations of the magnetic axes with respect to the crystallographic axes are shown in Fig. 8. The angle φ is calculated from Eq. (5b), assuming that the electric fields associated with the two Cu^{++} ions are tetragonal and identical except in orientation. Angles ψ and δ are directly measured (see Fig. 2).

B. Measured g Values

Rotating the crystal about its b - (or β -) axis (which is kept orthogonal to the magnetostatic field H), observing line positions and using Eq. (2) one finds the g values shown in Fig. 2. From this curve g_{α} and g_{γ} are obtained, and from the orientations at which maximum and minimum g values occur the orientations of the α - and γ -axes are

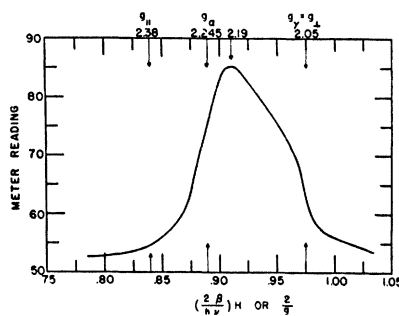


FIG. 6. Resonance absorption line in $\text{CuSO}_4 \cdot 5\text{H}_2\text{O}$ powder.

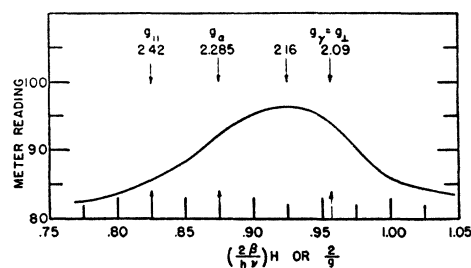


FIG. 7. Resonance absorption line in $\text{CuK}_2(\text{SO}_4)_2 \cdot 6\text{H}_2\text{O}$ powder.

¹⁴ J. H. Van Vleck (to be published), abstract in Phys. Rev. **73**, 1249 (1948).

¹⁵ D. M. S. Bagguley and H. E. Griffith, report, Nature **162**, 538 (October 2, 1948) that the two peaks are clearly resolved at a wave-length of 0.85 cm. Our results are in essential agreement with their 3-cm results.

¹⁶ W. Hofmann, Zeits. F. Krist. **78**, 279 (1931).

¹⁷ J. C. Hupse, Physica **9**, 633 (1942).

known. The value of g_{β} is then obtained by rotation about " γ ." With the help of Eq. (5b), g_{11} and g_{\perp} can then be calculated. These values are listed in Table I together with the splittings obtained from Eq. (4). Although the precision of the splitting values is very poor, it can be said that the splitting is less in the double salt than in the single salt.

C. Line Widths

Line broadening caused by magnetic dipolar interaction is evident in the absorption lines observed in $\text{CuK}_2(\text{SO}_4)_2 \cdot 6\text{H}_2\text{O}$. In Fig. 2 are shown line widths of the resonances observed when the β -axis is perpendicular to H . For these crystal positions the g values of the two Cu^{++} ions are mutually equal and the lines obtained are therefore single ones (cf. §III C). There is a line width maximum along the c -axis (400 gauss) and a sub-maximum along the a -axis (300 gauss). Between these directions there are minima of 150 gauss and 200 gauss.

The purely dipolar line width (no exchange interaction) as given by Van Vleck,¹³ is

$$\Delta H = \frac{h}{g\beta} \Delta \nu = 2.35g\beta \left\{ 3S(S+1) \sum_k r_{jk}^{-6} \left(\frac{3}{2} \cos^2 \theta_{jk} - \frac{1}{2} \right)^2 \right\}^{\frac{1}{2}}, \quad (8)$$

where j refers to any particular paramagnetic ion, k refers to neighboring paramagnetic ions, r_{jk} is the distance between ions j and k , and θ_{jk} is the angle between the magnetic field and the line joining ions j and k . Line widths calculated from this equation for several crystal orientations are plotted as filled circles in Fig. 2. (In the absence of x-ray data on $\text{CuK}_2(\text{SO}_4)_2 \cdot 6\text{H}_2\text{O}$, values of r_{jk} and θ_{jk} in $\text{MgK}_2(\text{SO}_4)_2 \cdot 6\text{H}_2\text{O}$ computed from Hofmann's data¹⁶ are used. See Table II.) The good quantitative agreement between observed and calculated line widths is a strong indication that there is very little exchange interaction between paramagnetic ions in this salt.

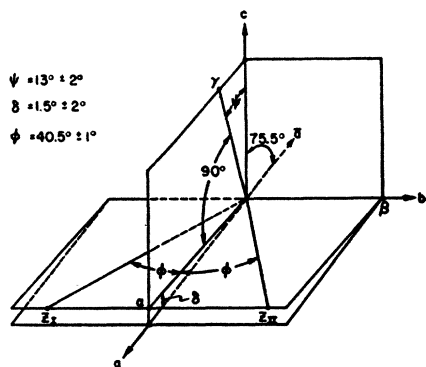


FIG. 8. Orientation of magnetic axes (α, β, γ) and crystallographic axes (a, b, c) in $\text{CuK}_2(\text{SO}_4)_2 \cdot 6\text{H}_2\text{O}$.

TABLE II. Spacing of magnetic ions in sulfates of copper.

	$\text{CuSO}_4 \cdot 5\text{H}_2\text{O}^*$	$\text{CuK}_2(\text{SO}_4)_2 \cdot 6\text{H}_2\text{O}^{**}$
	2 at 5.97A	2 at 6.1A
	2 at 6.12A	2 at 9.0A
CuI has CuI neighbors	2 at 7.16A	2 at 9.5A
	2 at 9.75A	2 at 12.1A
CuII has CuII neighbors	2 at 10.7A	2 at 12.2A
	2 at 11.1A	
	2 at 11.5A	
	2 at 5.55A	4 at 7.6A
	2 at 6.72A	4 at 9.0A
CuI has CuII neighbors	2 at 6.84A	4 at 10.5A
	2 at 8.86A	
	2 at 9.13A	
	2 at 9.26A	

* See reference 10.

** In the absence of x-ray data on this particular salt the spacings are assumed to be approximately those found in $\text{MgK}_2(\text{SO}_4)_2 \cdot 6\text{H}_2\text{O}$. Hofmann finds only a 4 percent variation in dimensions among a number of salts of the type $\text{XV}_2(\text{SO}_4)_2 \cdot 6\text{H}_2\text{O}$. See reference 16.

D. Effect of Exchange Coupling on Line Position

If the γ -axis is perpendicular to H , there should be some rotation positions at which a separate absorption peak for each Cu^{++} in the unit cell is observed (cf. §III D). In $\text{CuK}_2(\text{SO}_4)_2 \cdot 6\text{H}_2\text{O}$ this is actually the case, as is shown in Fig. 4. The arrows in the figure indicate expected positions of the separate peaks calculated from Eq. (6). Resolution of these two peaks shows that the exchange coupling between the paramagnetic ions is much less in the double salt than in the single salt, which is to be expected since the ions are closer together in the latter.

The fact that two peaks are obtained with " γ " normal to the external field proves that " γ " and not " α " is the axis normal to the plane of $Z_I Z_{II}$.

E. Absorption in Powder

The absorption line in powdered $\text{CuK}_2(\text{SO}_4)_2 \cdot 6\text{H}_2\text{O}$ (Fig. 7) has a maximum near $H(g_{\perp})$, corresponding to the weak coupling model (cf. §III E).

V. SUMMARY

Copper sulfate and copper potassium sulfate are similar in the following respects. In the unit cell of each there are two Cu^{++} ions, each ion located at the center of an electric field of approximately tetragonal symmetry. The axes of symmetry are oriented about 80° apart.

Dissimilarities in the magnetic properties of the two salts arise mainly from the difference in concentration of the paramagnetic ions. Denoting the two different Cu^{++} ions in the unit cell as CuI and CuII the spacings shown in Table II exist in the two salts.

The closer spacing in the single salt has two marked effects, both due to exchange coupling between the paramagnetic ions. In $\text{CuSO}_4 \cdot 5\text{H}_2\text{O}$:

(a) the absorption lines are much narrower than would be predicted by dipolar coupling considerations alone, and (b) for orientations of the crystal at which there should be separate lines for CuI and CuII , only one line is observed. The second effect depends upon exchange coupling of the type of CuI-CuII while the first depends upon any of the types, CuI-CuI , CuII-CuII , or CuI-CuII . Neither of these effects is noted in $\text{CuK}_2(\text{SO}_4)_2 \cdot 6\text{H}_2\text{O}$.

The difference in the magnitudes of the crystal-

line electric field splittings in the two salts is not related to exchange coupling, but is rather an indication that the octahedral water-oxygen complex is of smaller dimensions in the single salt.

ACKNOWLEDGMENT

The authors wish to express their gratitude to Professor J. H. Van Vleck for suggesting the importance of this problem and for many useful discussions of the results.

PHYSICAL REVIEW

VOLUME 75, NUMBER 8

APRIL 15, 1949

The Work Function of Lithium

PAUL A. ANDERSON

State College of Washington, Pullman, Washington*

(Received January 3, 1949)

Because they approximate their free electron models so closely, lithium and sodium are of exceptional importance in studies of the theory of the work function. For the purpose of supplementing theoretical calculations on these metals, a thorough experimental investigation of the work function of lithium has been carried out and the results, in combination with the calculations of Wigner and Bardeen, used to estimate the contribution of the surface double layer term to this work function.

As in previous studies of this series, the work function was determined by measurement of the contact difference of potential of lithium with respect to a barium reference surface of known work function. The measured surfaces of both lithium and barium were prepared by condensation of their

vapors on glass targets after each of the metals had been subjected to fractional and multiple distillation in the measuring tube itself. The time interval between deposition and measurement of the films was of the order of 30 seconds. The observed contact difference of potential is 0.03 ± 0.02 ev, lithium electro-positive to barium. This result assigns the value 2.49 ± 0.02 ev to the work function of lithium. The effect of gaseous contaminants is to lower the work function.

The volume and surface double layer terms which determine the work function of lithium are of the order of 2.2 and 0.3 ev, respectively, a result which supports the conclusion that the surface double layer makes a relatively small contribution to the work functions of the alkali metals.

A PROBLEM of major significance in work function theory and in surface physics generally is that of separating and evaluating individually the volume and surface terms which determine the external work function of a metal. Wigner and Bardeen¹ and Bardeen² have obtained equations of the form:

$$\phi = \phi_v + \phi_s = \phi_v + 4\pi e P_n,$$

where ϕ is the external work function which is measured experimentally. ϕ_v is the volume contribution to the work function and ϕ_s the contribution of the surface double layer. ϕ_v is determined entirely by the bulk properties of the lattice and may be defined as the work done in removing an electron from a hypothetical neutral lattice in which P_n , the surface dipole moment per unit area, is zero. ϕ_s contains all of the surface sensitive part of the work function, e.g., the dependence of ϕ on the crystal orientation of the surface. Neither ϕ_v

nor ϕ_s can be measured independently. Wigner and Bardeen¹ made rough calculations of ϕ_v for the free electron models of the alkali metals and by comparing their results with experimental values for ϕ reached the conclusion that ϕ_s is small, i.e., of the order of a few decivolts, for these metals. Bardeen² carried out a more complete evaluation of ϕ_v and also an explicit calculation of ϕ_s for sodium obtaining a calculated value for the work function which could be compared with the results of experimental measurements. These procedures evidently put a heavy burden on the experimental data. Examination of published work³ reveals a divergence in ϕ values, especially in the values for lithium, which is considerably larger than the probable magnitude of the double layer term which is to be evaluated and, in the case of lithium, no determination in which the experimental conditions now known to be essential were realized. The major objective in the present work was a thorough experimental study of lithium, a metal which approximates its free electron model quite exactly and

* Assisted by the ONR under Contract No. N6-ori-167.

¹ E. Wigner and J. Bardeen, *Phys. Rev.* **48**, 84 (1935).

² John Bardeen, *Phys. Rev.* **49**, 653 (1936). See Frederick Seitz, *Modern Theory of Solids* (McGraw-Hill Book Company, Inc., New York, 1940), pp. 395-400.

³ A. L. Hughes and L. A. DuBridge, *Photoelectric Phenomena* (McGraw-Hill Book Company, Inc., New York, 1932), p. 75.